HGF for Behavioural Analysis: Perceptual Model for Anxiety Patients During Lockdown

Francesco Branca, Davide Menini, Sara Sangalli
Emails: {fbranca, dmenini, sansara}@student.ethz.ch

***Abstract*—In this project we analyze via Hierarchical Gaussian Filtering (HGF) the relationship between State anxiety and the capacity of learning in a pool of subjects during COVID-19 lockdown. Eventually, we prove that all the subjects learn similarly in an impartial context, while they present clear differences in a psychologically involving context related to COVID-19. The analysis is performed through HGF estimations, K-means clustering, response simulations, and all the results are consistent with our expectations.**

I. Introduction

The COVID-19 pandemic has drawn people's attention towards a more accurate personal healthcare. This was initially reflected by the high request of hand sanitizers and soap at the beginning of the lockdown phase (8^{th} of March, 2020 in Italy). This anomalous situation has driven us towards the design of an experiment about anxiety in the very specific context of lockdown [1].

In this project we aim to analyze the relationship between State anxiety and the capacity of learning in 51 Italian subjects via Hierarchical Gaussian Filtering (HGF) [2] [3]. To reach this goal we have developed a visual-visual stimulus-stimulus learning [SSL] task structured in two tests, which try to simulate an impartial context, i.e. a neutral scenario where the subject should be able to learn the evolution of a stimulus sequence without any distraction, and a psychologically involving context, i.e. a disturbing scenario where the learning of the same sequence could be influenced by some psychological factors.

To acquire clinical relevance, we also propose the subjects a State-anxiety questionnaire based on the State-Trait Anxiety Inventory (STAI) [4], which labels them either as healthy controls or anxiety patients. This is useful as ground truth to validate our analysis.

The results of the STAI questionnaire and the responses of the two tests are analyzed through the HGF Toolbox [5] and K-Means clustering. In particular, we are interested in (1) the estimation of some perceptual parameters for each subject, (2) the clustering of these estimates into the two aforementioned groups (healthy controls and anxiety patients), (3) the simulation of the responses of an ideal anxiety patient and an ideal healthy control, whose parameters are defined by the clusters' centroids.

Eventually, we prove our hypothesis: healthy controls and anxiety patients have well distinguishable perceptual parameters for the psychologically involving context, while this distinction is not equally clear for the impartial context. In particular, healthy controls tend to learn faster than anxiety patients, which are more easily impressionable by a psychologically disturbing environment. These conclusions are supported both qualitatively, i.e. with plots of parameter spaces and HGF trajectory simulations, and quantitatively, i.e. with K-Means accuracy scores and user's test scores.

The following Sections explain the theory necessary to understand the basics of HGF and STAI (II), introduce the method of our analysis (III), provide details on the implementation (IV), show the results (V) and draw conclusions (VI).

II. Theoretical Background

A. The Theory of Bayesian Brain

Learning can be seen as the process of updating an agent's beliefs about the world by integrating new and old information. This allows humans to base predictions on past experiences, consequently improving their actions.

In order to understand how biological agents learn, there are two possible approaches. The first one is bottom-up and it is built on the neuronal architecture of synapses and brain circuits. A second approach is top-down, using generic computational basis to build generative models of learning, to infer on the underlying mechanisms [6]. The latter approach is the one that we employ in our project.

One of the main aspects about the capability to infer about the states of the world is how the brain is influenced by both prior beliefs and incoming cues from the physical observed reality. Moreover, the received sensory information, which agents base their decisions on, are typically noisy and incomplete, hence not fully accurate and reliable. Therefore, to understand perception and the representations of the world built by the brain, it is crucial to take into account causal and statistical relations as a foundation basis.

Starting from these considerations, Bayesian statistics has become more popular in neuroscience, which started to exploit it to mathematically model problems of inference and decision-making under uncertainty.

The theory of Bayesian Brain is based on the idea that our brain updates its beliefs on the world based on the Bayes' theorem, which states the following:

$$p(x|y) = \frac{p(x) \cdot p(y|x)}{p(y)}, \tag{1}$$

where the "posterior" $p(x|y)$ is the inference on belief about the states of the world *x(t)*, given sensory inputs y(t). This quantity is proportional to:

- The 'prior' $p(x)$, which is the prior belief on the states of the world, before receiving the sensory input.
- The 'likelihood' $p(y|x)$ which is how likely is the observation given the real states of the world. This represents the generation of sensory inputs.

In general, there is not certainty on the prior and posterior probabilities and assumptions can be done on the generation of sensory inputs. Any Bayesian learning scheme relies upon the definition of a so-called 'generative model', which is a set of probabilistic assumptions about how sensory signals are generated. Our approach makes use of a framework which assumes that agents have an internal generative model of their sensory input [3]. This model is generative in the sense that it describes sensory inputs as regenerated by the external world. It does this by assigning a probability (the likelihood) to each sensory input given states - which vary with time - and parameters - which are constant in time - and by completing this with a prior probability distribution for states and parameters. It is described by the following:

$$p(x, y|m) = \frac{p(x) \cdot p(y, x|m)}{p(y|m)} \tag{2}$$

While the purpose of the model is to predict input coming from the external world, it is internal in the sense that it reflects the agent's beliefs about how sensory inputs are generated by the external world.

B. Hierarchical Predictive Coding

Predictive coding is a theory according to which the brain is constantly generating and updating a hierarchical generative model of the environment. The model is used to generate predictions of sensory inputs that are compared to the actual states of the world. This comparison is called prediction error and it is defined as: $\mu_{\text{lkd}} - \mu_{\text{prior}}$. It changes inversely with the beliefs likelihood: the greater the likelihood of hypothesis, the smaller the prediction error generated.

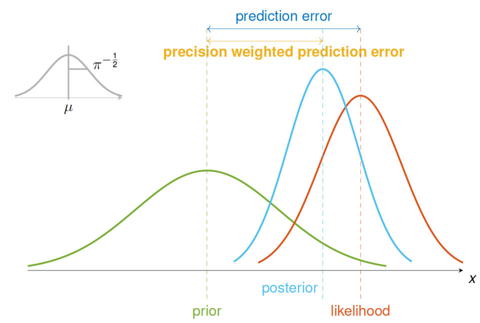

Fig. 1: Conditional Gaussian probabilities used for calculating precision weighted prediction error.

More precisely, during the process of Bayesian inference on the posterior, the brain performs the so-called precision-weighted Prediction Error Minimization (PEM).

According to this model, expectations about the precision (π) or "inverse variance" of incoming sensory inputs are crucial for effectively minimizing prediction error. The expected precision of a given prediction error can inform confidence in that error, which influences the extent to which the error is weighted in updating predictions [7]. This setup is depicted by Figure 1 .

This process of weighting the prediction error is modelled in the following way:

$$\pi_{\text{posterior}} = \pi_{\text{prior}} + \pi_{\text{lkd}} \tag{3}$$

$$\mu_{\text{posterior}} = \mu_{\text{prior}} + \frac{\pi_{\text{lkd}}}{\pi_{\text{posterior}}} \cdot (\mu_{\text{lkd}} - \mu_{\text{prior}}) \tag{4}$$

The ratio of precision then determines the learning rate: the higher the precision of the priors relatively to incoming information, the lower the learning rate and therefore the less the prediction error influences the posterior and vice versa. In summary, the more an agent knows about a topic, the lower the uncertainty of the prior, and the prediction errors is weighted less in formulating inference.

C. Hierarchical Gaussian Filtering (HGF)

The Bayesian learning model, as described in [2], relies on the definition of 'generative model', inspired in turn by [8]. A generative model was defined by Mathys et al. as a set of probabilistic assumptions on how a signal is generated. Such a model is called 'hierarchical' when it is composed of a vertical structure of states, described by time-dependent variables that evolve in time as a random walk. Those hidden states are the ones that control the contingencies in the environment.

In this section, we describe a specific version of the Bayesian learning model called Hierarchical Gaussian Filter (HGF).

In the hierarchy of states, we need to introduce a form of volatility coupling between the layers. This general concept has been used in various applications. In principle, there can be many forms of coupling where high levels influence the parameters of the lower states. In our case, the bound parameter is the variance, but many other different update equations can be derived. The coupling between the layers can be any function: in the HGF model the state variables are mapped between each other by Gaussian distributions, where the walk's step size of a level (i.e. the variance of the Gaussian distribution) is determined by the next highest level of the hierarchy.

In a generative scenario, the agent's environment is conveying sensory inputs. This is based on a quite simple assumption: there might be a quantity in the world, e.g. x_1, that is changing over time. By tracking this value, given the sensory input, we may want to infer its next value. This is exactly what the agent is asked to do, based on his belief about the world. The probability of observing a value of x_1 at some point is a normal distribution characterized by some variance and by a mean, that is the previous value of the state. There might be a higher-level state in the world, e.g. x_2, that might determine the step size (i.e. the variance of x_1). If the higher level quantity changes, the speed of the lower level quantity (i.e. 'volatility') changes as well. The more volatile a certain state in the world is, the faster the changes are. For example, seasons change can be described as the highest state, where the daily temperature is the lower level. The temperature during the day might change faster or slower depending on the upper level.

Even though HGF model could be easily extended to complex environments, the model proposed by [2] deals with a simple scenario, where the sensory input $u(k) \in \{0, 1\}$ at time k is in a binary form. In our model, similarly to [3], the agent is provided with a single two-states random variable of the environment, e.g. a picture that represents two possible conditions, controlled by a binary random variable. In particular, at step k, the environmental state x_1 determines the outcome of the sensory input u that is received by the agent. For simplicity the index k is omitted. At first instance, a deterministic form of the likelihood is assumed:

$$p(u|x_1) = (u)^{\mathrm{x}_1}(1-u)^{1\text{-}\mathrm{x}_1} \tag{5}$$

If $x_1 = 0$, then the probability $p(u = 0|x_1 = 0) = (1-u) = 1$, that is $u = 0$. Similarly, if $x_1 = 1$, then $u = 1$ with probability of 1. In this simple model, u can be accurately predicted (in a deterministic way) from x_1. This basic assumption will later be replaced by a probabilistic mapping (better explained in Section IV), with the scope of introducing perceptual uncertainty to the agent. We recall that the concept of HGF allows to change the levels' coupling function without loss of generality.

The probability of x_1, being binary itself, can be described by a random number, represented by the next upper level in the hierarchy, i.e. $x_2 \in \mathbb{R}$, an unbounded real parameter of $p(x_1)$ that is mapped by a sigmoid function (softmax) to the range [0,1]. The mapped probability value of x_2 is used as a parameter for the Bernoulli distribution, to get the probability distribution of x_1:

$$\begin{aligned} p(x_1|x_2) &= s(x_2)^{\mathrm{x}_1}(1-s(x_2))^{1\text{-}\mathrm{x}_1} \\ &= Bernoulli(x_1; s(x_2)) \end{aligned} \tag{6}$$

where $s(x)$ is the sigmoid function:

$$s(x) = (1 + \exp(-x))^{-1} \tag{7}$$

According to the generative model, the probability of x_2 changes with time as a Gaussian random walk. The value of x_2 at time k is normally distributed, with the mean at its previous value ${x_2}^{(\text{k-1})}$ and variance (i.e. 'dispersion of random walk') that depends exponentially on the upper level x_3 and the parameters κ and ω. In this model, x_3 determines the log-volatility of the environment, as stated in [8]

$$\begin{aligned} p({x_2}^{(\text{k})}|{x_2}^{(\text{k-1})}, {x_3}^{(\text{k})}) = \\ \mathcal{N}({x_2}^{(\text{k})}; {x_2}^{(\text{k-1})}, \exp(\kappa {x_3}^{(\text{k})} + \omega)) \end{aligned} \tag{8}$$

Similarly, also x_3 performs a Gaussian random walk. This concept can be repeated for an arbitrary number of layers. In this project, there are only three default levels, thus the volatility of x_3 (the highest level) is fixed and parameterized by the constant θ:

$$p({x_3}^{(\text{k})}|{x_3}^{(\text{k-1})}, \theta) = \mathcal{N}({x_3}^{(\text{k})}; {x_3}^{(\text{k-1})}, \theta)) \tag{9}$$

Finally, the full levels' hierarchy of the generative model can be written as a recursive function for all times k, starting from $k = 1$. Given the initial values of states and the priors on the parameters $p(\kappa, \omega, \theta)$, the variables' distributions of the next state are generated from the following equation:

$$\begin{aligned} &p(u^{(\text{k})}, {x_1}^{(\text{k})}, {x_2}^{(\text{k})}, {x_3}^{(\text{k})}, {x_2}^{(\text{k-1})}, {x_3}^{(\text{k-1})}, \kappa, \omega, \theta) = \\ &p(u^{(\text{k})}|{x_1}^{(\text{k})}) \cdot p({x_1}^{(\text{k})}|{x_2}^{(\text{k})}) \cdot p({x_2}^{(\text{k})}|{x_2}^{(\text{k-1})}, {x_3}^{(\text{k})}, \kappa, \omega) \cdot \\ &\cdot p({x_3}^{(\text{k})}|{x_3}^{(\text{k-1})}, \theta) \cdot p({x_2}^{(\text{k-1})}, {x_3}^{(\text{k-1})}) \cdot p(\kappa, \omega, \theta) \end{aligned} \tag{10}$$

To summarize, the model can be described by the following parameters, that characterize the two highest layers x_2, x_3:

- μ_2, μ_3: initial means of x_2, x_3 at $k = 0$
- $\sigma_1, \sigma_2,$: initial variances of x_2, x_3 at $k = 0$
- ω_1, ω_2: default volatility of x_2, x_3
- κ_2: coupling parameter of x_2 and x_3

We have described how the environmental states can be obtained recursively via the generative model, and how knowing them allows for an accurate prediction of input u. Given the generative model, the probability theory provides the optimal solution on how the agent can make best use of the previous inputs $u(1), ..., u(k-1)$ and other priors, to predict the next input $u(k)$. In order to perform the prediction task, the model has to be fitted by the agent. Inverting the model corresponds to optimize the posterior densities of the hidden states (x_1,x_2,x_3) and parameters of the model (k,θ,ω). This inversion or 'fitting' of the model enables to derive the update equations for the posterior expectations of the hidden states. According to [2] optimizing the posterior densities over the states x corresponds to perform perceptual inference. This optimization can be carried out either by exact inversion [8] or by variational Bayesian inversion as in [9] and [10]. The resulting model is referred to as the 'perceptual model' of the agent.

D. *State-Trait Anxiety Inventory (STAI)*

The State-Trait Anxiety Inventory (STAI) is a psychological inventory based on a 4-point scale and it consists of 40 questions on a self-report basis. It was developed by psychologists Charles Spielberger, R.L. Gorsuch, and R.E. Lushene and its most current revision is Form Y, which is the version we decided to adopt for our assessment [11] .

The STAI is a test/questionnaire that shows how strong a person's feelings of anxiety are and it measures two types of anxiety – state anxiety, or anxiety about an event, and trait anxiety, or anxiety level as a personal characteristic. For the purpose of this project, we are interested in the State anxiety (S-anxiety), which can be defined as fear, nervousness, discomfort, and the arousal of the autonomic nervous system induced by different situations that are perceived as dangerous [4]. This type of anxiety refers more to how a person is feeling at the time of a perceived threat and it is considered temporary.

The two forms of anxiety are separated in the inventory, and both are given their own 20 separate questions. For the purpose of our project, we only employ those related to S-anxiety.

Scores range from 20 to 80, with higher scores correlating with greater anxiety. The 4-point scale for S-anxiety is as follows: 1.) not at all, 2.) somewhat, 3.) moderately so, 4.) very much so.

III. Method

Our idea is to propose two tests to the subjects, simulating two scenarios:

- *Impartial context*: in this test the subjects are exposed to a neutral scenario, where ideally there isn't any preference or concern about the topic.
- *Psychologically involving context* during COVID-19 lockdown: in this test the subjects are exposed to a possibly upsetting scenario, where they may be biased towards a certain belief based on their clinical conditions.

These are the two behavioural tasks we are going to take into account in our analysis.

Moreover, a third test consisting of 20 questions from the 'State-Trait Anxiety Inventory' [11] is used as ground truth to validate our data.

In the following sections we are going to describe more in details these tests and the analysis performed on the obtained responses. Figure 2 provides an overview of our experiment flow.

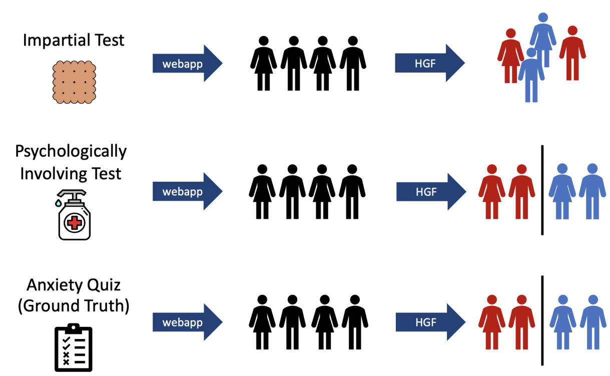

Fig. 2: Experiment flow.

A. *Experiment Design*

An associative learning task (visual-visual stimulus-stimulus learning [SSL]) is used, where participants have to learn the same binary sequence of visual cues and predict a subsequent visual stimulus in the two contexts.

In both scenarios, the participants imagine to be in a daily situation at the supermarket, where they have to buy a certain good, which may or may not be present there. After being provided with this information, they are asked to guess whether the same good is present or not in a nearby supermarket and they are finally shown the correct answer. Figure 3 provides an example of trial.

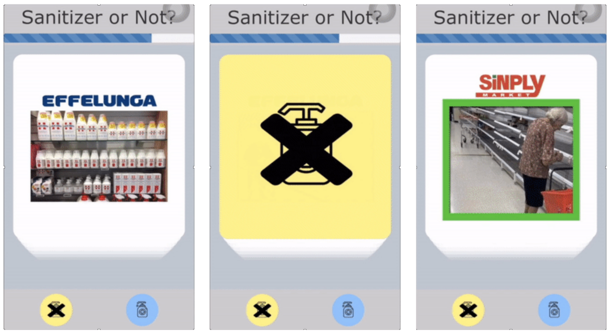

Fig. 3: Webapp interface for the psychologically involving test. (1) Visual cue: full shelves, (2) Agent's decision: no sanitizers, (3) Correct outcome: empty shelves.

The input information is provided as visual cues, which are displayed for 5 seconds. Within this time, the subjects have to signal their prediction by button press. Eventually, if the agents' response is right the correct outcome is shown for 3 seconds, otherwise they are reported of the error and no visual outcome is shown. If the response is not provided within the response time, the outcome is registered as non-valid.

Both tests use the same binary sequences of visual cues and correct outcomes: the latter are generated via a generative model, the former are generated backwards via a Bernoulli distribution of the correct outcomes. The input sequences are required to be equal across the tests in order to perform an objective comparison of the responses. More details are given in Section IV.

The fundamental difference between the tasks concerns the involved good: (1) biscuits for the impartial context, (2) hand sanitizers for the psychologically involving one. We picked such products because usually they are equally reachable by the subjects in their daily life, but in the COVID-19 lockdown they are given a different value. This choice should allow them to better identify themselves with the situation.

Some general remarks about the tests: (1) each test is composed of 120 trials; (2) after half of the test duration (60 trials) the response time is changed to 4 seconds, and the visualisation time of the correct outcomes is changed from 3 to 2 seconds; (3) the order in which the tests appear to the agents is randomized to avoid bias in the results due to loss of concentration in the last test.

The anxiety questionnaire is composed of 20 questions related to State anxiety. They are taken from STAI Form Y [11], but questions where anxiety is originally absent (e.g. 'I feel calm') are inverted (e.g. 'I don't feel calm') in order to make the scoring system less complicated. Even though the questionnaire results in one out of multiple anxiety levels, we are only interested in a binary separation, i.e. anxiety patients or healthy controls. Eventually, this binarized outcome is used as ground truth to validate our analysis, which is tackled in Section III-C.

B. Subjects

For the purpose of the project, we build our own dataset. The experiment is carried out on 51 Italian subjects, who have always stayed in Italy for the duration of the COVID-19 lockdown (i.e. from the 8th of March onwards). Thanks to the user-friendly web-application we manage to reach quite a diverse pool of users:

- 59% women, 41% men
- Age comprised between 20 to 63 years old

The participants do not present any psychiatric or neurological disorders in their past medical history.

C. Response Analysis

The agents' responses for the two tests are labeled as 'anxiety patients' or 'healthy controls', depending on the result of the anxiety questionnaire. This allows to have a ground truth for the impartial and psychologically involving contexts, useful to validate the analysis.

Firstly, an estimation of some perceptual parameters for each context is carried out. In particular, the analysis is performed on the following parameter configuration, proposed during the exercise session: ω_2, ω_3, μ_3. This estimation leads to two 3D parameter spaces, one for each context, where a point is a triplet (ω_2, ω_3, μ_3).

Another matter of interest is the correlation between the parameters. If the parameters are not fully correlated, they are said to be independently identifiable, which means that their variations are independent. This is the ideal situation for a 3D parameter space, since otherwise the information on one axis would be redundant and it could be discarded.

Next, K-Means clustering is used to divide the point clouds in two clusters, namely healthy controls and anxiety patients. Then, by comparing the K-means outcomes to the ground truth, the accuracy of the clustering algorithm is calculated for both contexts.

Furthermore, the coordinates of the healthy and anxious clusters' centroids for the psychologically involving context are used to simulate and compare the behaviour of two ideal anxious and healthy agents. This comparison is performed both qualitatively, i.e. with plots of the simulated responses, and quantitatively, i.e. with the percentage of correct answers.

We also simulate the response of an optimal agent, whose perceptual parameters are obtained from an estimation using a Bayesian optimal response model. These parameters are the ones that produce the least cumulative Shannon surprise for a given input sequence. This means that an agent using this parameter setting would experience the least possible surprise when exposed to the given inputs under the given perceptual model.

In addition, we carry out mean and variance analysis on the estimates for the healthy controls and anxiety patients, accordingly to the ground truth.

In order to generalise our analysis, we also try out some other configurations of parameters: (ω_2, κ_2, μ_3), (ω_3, κ_2, μ_3) and (ω_2, ω_3, κ_2).

IV. Implementation

A. Input Generation

Both the impartial and the psychologically involving tests use the same input sequences of cues and correct outcomes. The employed sequences are depicted in Figure 4. They are related by a probability of correct outcomes given cues $p(out|cue)$, which is defined as a step function with values [0.1 0.9 0.3 0.7 0.1 0.9], where each step is 20-trials long.

The correct outcomes are produced by a generative model with 3 levels:

- ${x_3}^{\mathrm{k}} \sim \mathcal{N}({x_3}^{\mathrm{k\text{-}1}},\, exp(\omega_3))$
- ${x_2}^{\mathrm{k}} \sim \mathcal{N}({x_2}^{\mathrm{k\text{-}1}},\, exp({x_3}^{\mathrm{k}} \cdot \kappa_2 + \omega_2))$
- ${x_1}^{\mathrm{k}} \sim Bernoulli(s({x_2}^{\mathrm{k}}),\, p(out|cue))$

The correct outcomes are the binary version of x_1:

$$out = round(x_1)$$

The cues are produced backwards by a Bernoulli distribution of the correct outcomes:

$$cues \sim Bernoulli(out,\, p(out|cue))$$

Eventually, the generated binary sequences are fed to the web-app, where they are associated with images to create the visual stimuli.

B. Data Sourcing

The crowd-sourced dataset is collected from an online experiment, delivered to the subjects as a responsive web application. The app is designed specifically to be shareable with no need for installation. This format allows us to reach a broad pool of potential users.

The interface presented to the user is simple, yet intuitive. First of all, a tutorial is shown to introduce the test and to let the user familiarize with the interface. A progress bar on the top shows the remaining time for each step. In a card stack-like interface, a pile of pictures shows the current visual cue in the middle of the screen, while the following cues are loaded in the stack. The user has to predict the next visual stimulus, either with the press of two buttons or by swiping left/right. This allows the subject an instantaneous reaction and the app can be used with one hand. At the end of each of the two tests, the score is presented to the user. Finally, after the completion of the whole experiment, the anxiety questionnaire is performed, providing the user with insights into his level of State anxiety.

The different tasks are designed as HTML pages, one for each test. The pages are loaded dynamically with a JavaScript file that generates the frame containing the visual cues and presents it to the user. Moreover, the script controls the timing and user interactions (button press and swipes).

At the end of the experiment, the user's input sequences are inserted into a Parse database. This allows to run the website on a static HTTP server, with no need for a dynamic back-end server. The web-app is tested and optimized for iOS and Android mobile devices.

The output table, containing the users' responses, is later exported from the Database as a JSON file and it is directly fed into the MATLAB pipeline, discussed in the following Sections.

C. Parameter Estimation

The function `tapas_fitModel` from the HGF Toolbox [5] fits the parameters of a combination of perceptual and observation models, given inputs u and responses y:

- Since the agent is learning a cue-outcome contingency, the input u is a composite event, i.e. it is coded in a contingency space.
- The perceptual model is the three level HGF for binary inputs (`hgf_binary`); it describes the states or values that probabilistically determine the observed responses.
- The response model is the unit-square sigmoid decision model with a readout of μ_3 (`unitsq_sgm_mu3`); it describes how the states or values of the perceptual model map onto responses.
- The optimization algorithm used is `quasinewton_optim`; it determines the maximum-a-posteriori (MAP) estimates of the parameters of both the perceptual and decision models.

We use `fitModel` to estimate ω_2, ω_3, μ_3 for both the impartial and the psychologically involving contexts. The `fitModel` function is also used to find the 'Bayes optimal' perceptual parameters under the binary HGF model, i.e. the particular parameter values that produce the least cumulative Shannon surprise for a given input sequence u.

The correlation of the parameters is analyzed by using `tapas_fit_plotCorr`. This is only done for a small subset of agents, namely one anxiety patient and one healthy control.

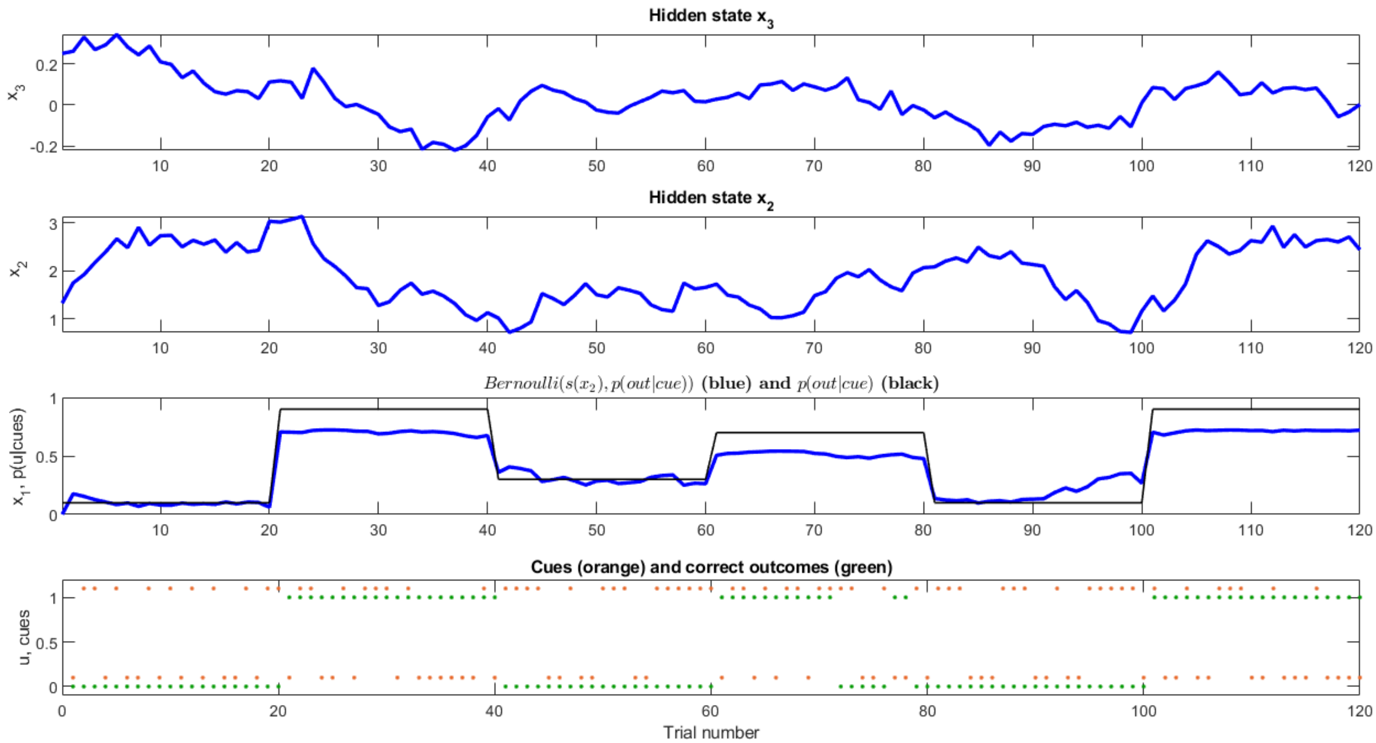

Fig. 4: Input generation: generative model states (blue), cues (orange) and correct outcomes (green).

D. Clustering

The estimates of the parameters ω_2, ω_3 and μ_3 for the two contexts are given as input to a K-Means clustering algorithm to determine two clusters: healthy controls and anxiety patients. Here we use the MATLAB function `kmeans()`, which returns both the cluster labels of the estimates and the positions of the $K = 2$ centroids.

By comparing the clusters to the ground truth, we also calculate the accuracy scores of the K-means: a score of 0.5 means that the separation is random and it is the minimum value allowed.

E. Simulation

The function `tapas_simModel` from the HGF Toolbox [5] simulates responses from a combination of perceptual and observation models, given parameters and inputs u. To keep consistency throughout the analysis, the models are the same as the `fitModel` function (`hgf_binary` and `unitsq_sgm_mu3`). The parameters are set as follows:

- μ = [NaN, 0, $\hat{\mu_3}$]
- σ = [NaN, 1, 1]
- κ = [1, 1]
- ω = [$\hat{\omega_2}$, $\hat{\omega_3}$]

We use `simModel` to simulate the responses of a Bayesian optimal subject, an ideal anxiety patient and an ideal healthy control for the psychologically involving context. Depending on the simulation we are interested in, the estimated parameters ($\hat{\mu_3}$, $\hat{\omega_2}$, $\hat{\omega_3}$) are respectively set to either the values of the optimal parameters, the anxiety patients' centroid or to the healthy controls' centroid.

Moreover, by comparing the simulated responses to the correct outcomes, we calculate the involving test score for the ideal anxiety patient and the ideal healthy control.

V. Results

A. Parameter Estimation

The heart of our analysis consists of the estimation of the three aforementioned perceptual parameters. Figure 7a, in the left column, shows the parameter spaces obtained for the impartial and psychologically involving contexts. Each point is a triplet (ω_2, ω_3, μ_3) for an agent and it is labeled as either anxiety patient (in orange) or healthy control (in blue), accordingly to the ground truth. It is possible to notice that in the psychologically involving scenario the subjects of the two groups are arranged in a couple of relatively visible regions, while the impartial one presents a point-cloud-like distribution.

At the same time, we are interested in the correlation between the estimated parameters (Figure 5) for the different configurations of agents and contexts. Remarkably, the correlation is comprised between 0 and 0.7 in all the cases, meaning that these parameters are independently identifiable. Hence, the information in the parameter space is never redundant.

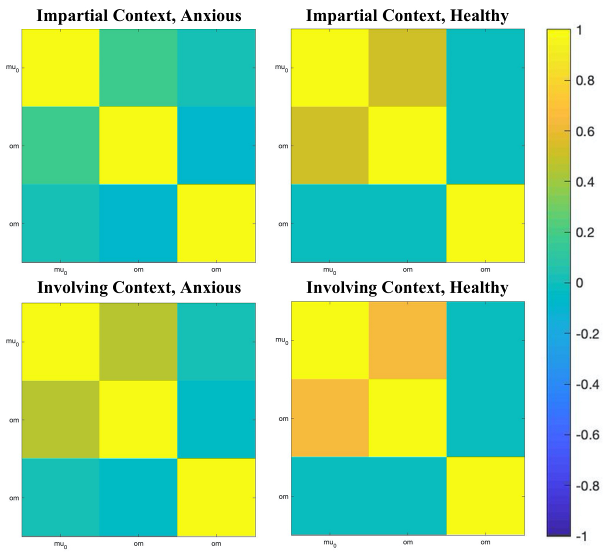

Fig. 5: Parameter correlations of $\omega_2, \omega_3, \mu_3$ for different configurations.

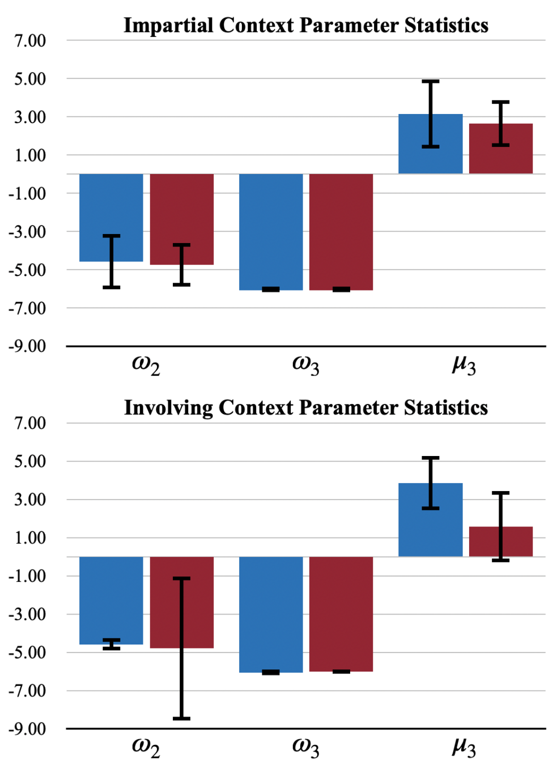

Fig. 6: Parameter statistics. The bar graphs show the mean value of each parameter for the healthy controls (blue) and anxiety patients (red) with the corresponding variance range (black).

Finally, we provide an insight into the statistics of the estimated parameters, in Figure 6. Supporting what is shown in Figure 7a, ω_3 is the parameter with the smaller variance, which means that its estimates are very close to the mean value with a satisfactory precision. Noticeably, ω_2 in the involving context for anxiety patients presents a variance ten times greater than the one for healthy controls.

B. Clustering

Starting from the estimation of the parameters, K-means clustering is performed to investigate to what extent the two analysed group are distinguishable between each other in the different contexts. The results of the clustering for the two scenarios, together with the respective ground truth, are shown in Figure 7a.

On the one hand, in the parameter space of the impartial context the subjects are arranged in a point-cloud-like scheme, accordingly to the ground truth. Consequently, the clustering algorithm performs poorly in separating healthy controls from anxiety patients, leading to an accuracy of 50.9%.
On the other hand, in the parameter space of the psychologically involving test the agents' responses are more separable into two distinguished groups. This is translated into the better clustering accuracy of 76.4%.

Overall, anxiety patients present lower volatility, when compared to the healthy controls.

In addition, the point corresponding to the Bayesian optimal parameters is represented with a green diamond: in both scenarios it falls into the the cluster of healthy controls.

C. Simulation

We aim at analysing and comparing the behaviour of the ideal healthy control and the ideal anxiety patient by simulating the perceptual model with the centroids' coordinates of the clusters as parameters. The simulated responses are displayed in Figure 7b: at the top the anxious subject, at the bottom the healthy one.

Looking at the posterior expectations of input $s(\mu_2)$, shown in red in the graphs, it is possible to notice that for the ideal healthy control it follows the cues distribution more quickly and deeply than anxiety patients. This finding is consistent with the trend of the respective learning rates: anxiety patient's one is nearly always flat, while healthy control's rate fluctuates more.

From a more quantitative point of view, these considerations are reflected on the obtained scores (percentage of correctly guessed trials): 50% for the healthy control and a lower 47.7% for the anxiety patient.

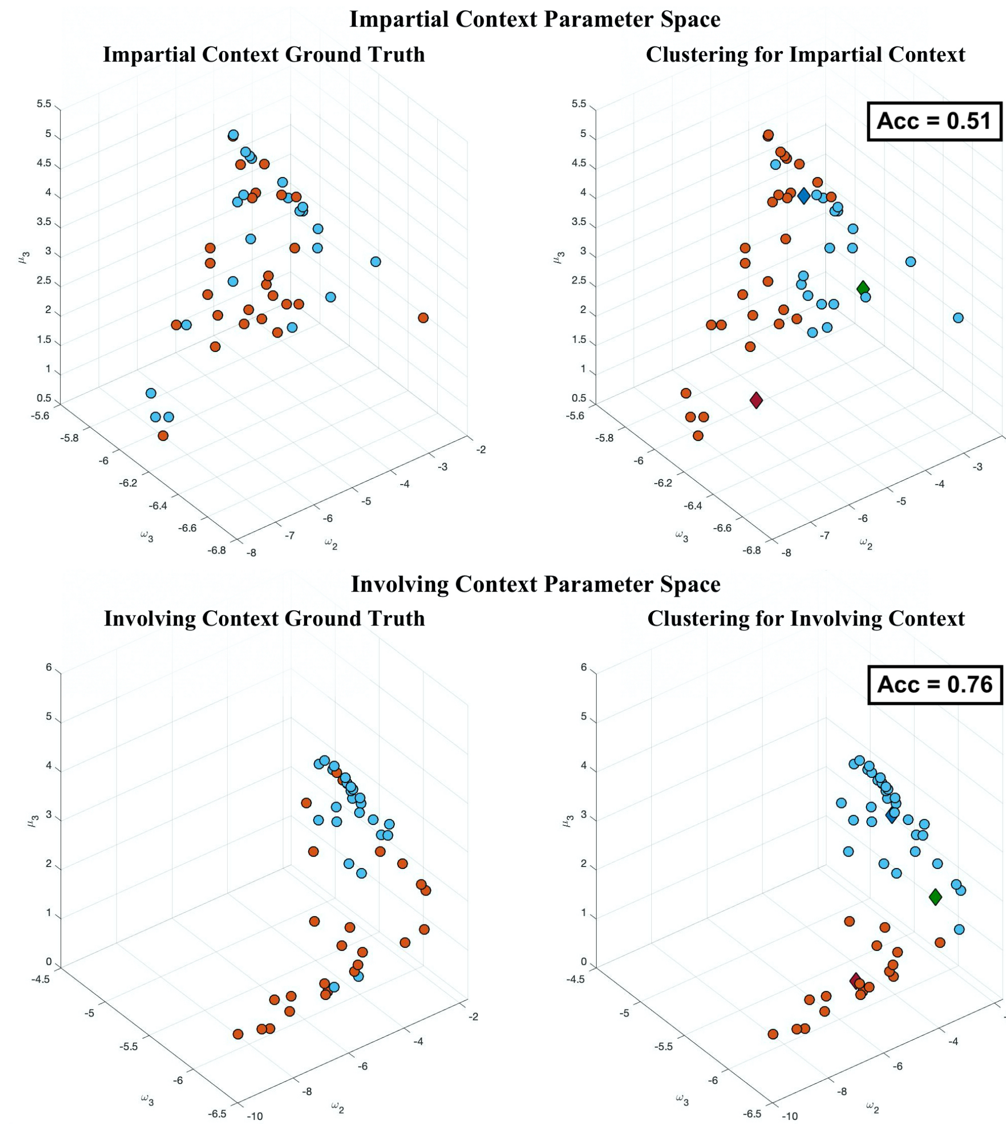

(a)

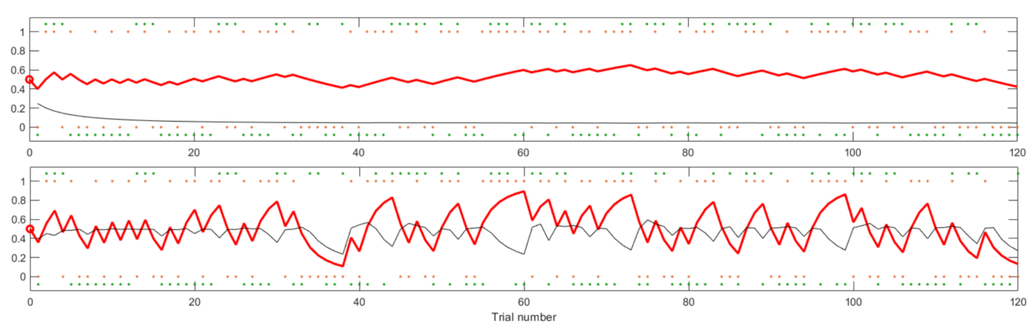

(b)

Fig. 7: (a) Ground truth and K-Means Clustering results for the impartial and psychologically involving contexts. Healthy controls (blue) and anxiety patients (orange) are shown with the respective centroids (diamonds) and the Bayesian optimal parameters (green diamond).
(b) Simulation of the ideal anxiety patient (top) and ideal healthy control (bottom). Response y (green), cues (orange), learning rate (fine black), and posterior expectation of input $s(\mu_2)$ (red) are represented.

We also simulate the response of an optimal agent, whose perceptual parameters are obtained from an estimation using a Bayesian optimal response model. These results are shown in Figure 8. The response of the ideal model is visibly similar to the one of the ideal healthy control. This confirms the results obtained from the clustering outcome analysed in Section V-B, where the point representing the optimal Bayesian model falls in the range of healthy controls.

D. Other Configurations

For the sake of completeness, we try to estimate different configurations of parameters.
Figure 9 shows the parameter spaces for the three new configurations, each with ground truth and cluster result for both impartial and psychologically involving contexts. Table I shows the K-means clustering accuracy scores for the two contexts. Configuration 1 is the one used throughout the complete analysis. While most of the configurations present the same accuracy Δ of 25%, Configuration 1 has better correlations (w.r.t. the analysed samples, not shown here).

	Parameters	Impartial	Involving
(1)	$\boldsymbol{\omega_2, \omega_3, \mu_3}$	51%	76%
(2)	$\omega_3, \kappa_2, \mu_3$	61%	86%
(3)	$\omega_2, \kappa_2, \mu_3$	65%	86%
(4)	$\omega_2, \omega_3, \kappa_2$	55%	80%

TABLE I: K-Means Clustering accuracy.

		Healthy		Anxious	
Parameters		*mean*	*var*	*mean*	*var*
(1)	ω_2	-4.582	0.337	-4.792	3.767
	ω_3	-6.078	0.010	-6.006	0.087
	μ_3	3.853	1.421	1.572	1.864
(2)	ω_3	-5.979	0.002	-6.025	0.015
	κ_2	0.281	0.003	0.596	0.639
	μ_3	3.952	1.215	1.892	1.437
(3)	ω_2	-3.684	0.121	-4.524	2.702
	κ_2	0.3754	0.005	0.633	0.1772
	μ_3	3.940	1.345	1.552	1.748
(4)	ω_2	-7.668	2.201	-5.203	3.325
	ω_3	-5.957	0.003	-6.028	0.009
	κ_2	0.334	0.063	0.467	0.092

TABLE II: Parameter statistics for the different configurations in the psychologically involving context.

Table II shows mean value and variance of the different parameter estimates for the psychologically involving context. The analysis is performed on healthy controls and anxiety patients separated accordingly to the ground truth. For the new configurations we can observe the same behaviour as Configuration 1, better shown in Figure 6: variances tend to be greater for the anxiety patients than for the healthy controls in the involving context, which means that they are more spread into the parameter space.

VI. Conclusion

The results presented in Section V confirm the initial hypothesis that all the subjects learn similarly in an impartial context, while they present clear differences in a psychologically involving context related to COVID-19.

In particular, we proved that healthy controls and anxiety patients' behaviours are different enough to become distinguishable by the K-Means Clustering only in the psychologically involving scenario. This does not happen in the impartial context, where the clustering algorithm has proved to be unable to discriminate between the two groups. This different behaviour is also visually confirmed by the plots of the parameter spaces in Figure 7a and by the resulting accuracy scores.

At the same time, looking at the simulations of the ideal healthy control and anxiety patient in Figure 7b, it is clear that the healthy patient is able to follow more carefully and dynamically the cues' sequence, when compared to the anxiety patient. This is also proved by the scores obtained from the simulations, which lead to the conclusion that healthy controls are able to learn better and more quickly than anxiety patient. An additional evidence for this is provided by the values obtained for μ_3 (more remarkably than the other parameters). Overall, healthy controls present higher values, which in turn translate into a higher volatility, and into a greater adaptability to the context, i.e. better learning capacity. Conversely, anxiety patients are more easily impressionable by a psychologically disturbing environment and consequently tend to adapt less efficiently to the presented context.

Moreover, since the Bayesian optimal parameters fall into the healthy controls' cluster, they are less exposed to the Shannon surprise: an healthy control would experience less surprise when exposed to the environmental stimuli under the given perceptual model than anxious patients.

VII. Contributions

We hereby declare that all group members (Branca Francesco, Menini Davide, Sangalli Sara) have equally contributed to the present project.

We would like to thank all our friends and relatives that offered to take part in our experiments.

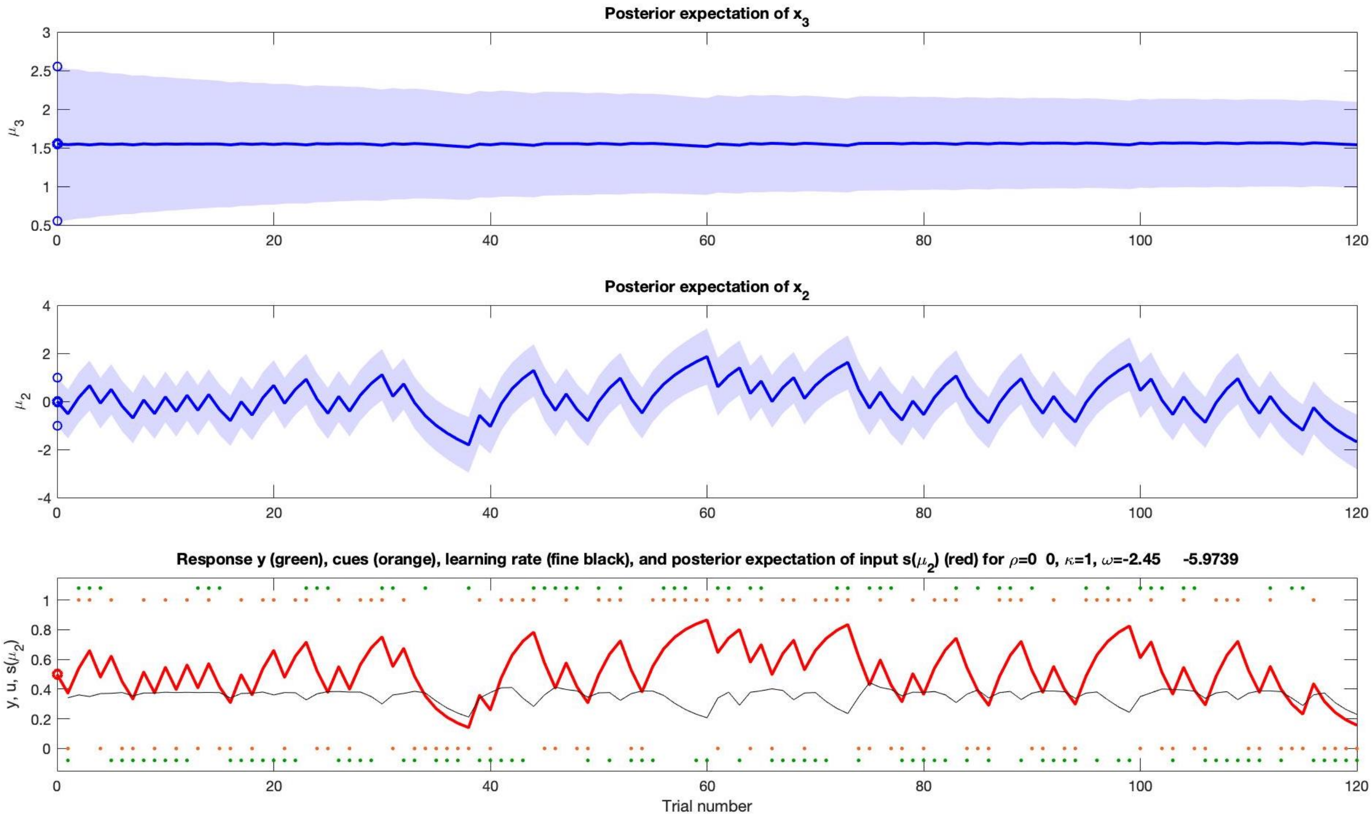

Fig. 8: Simulation of the Bayesian optimal model.

REFERENCES

[1] Forbes, "The entire country of italy is on lockdown because of the coronavirus," https://www.forbes.com/sites/rachelsandler/2020/03/09/the-entire-country-of-italy-is-on-lockdown-because-of-the-\coronavirus/, 2020.

[2] C. Mathys, J. Daunizeau, K. Friston, and K. Stephan, "A bayesian foundation for individual learning under uncertainty," *Frontiers in human neuroscience*, vol. 5, p. 39, 05 2011.

[3] C. Mathys, E. Lomakina-Rumyantseva, J. Daunizeau, S. Iglesias, K. H. Brodersen, K. Friston, and K. Stephan, "Uncertainty in perception and the hierarchical gaussian filter," *Frontiers in human neuroscience*, vol. 8, p. 825, 11 2014.

[4] P. Foley, B. Hartman, A. Dunn, J. Smith, and D. Goldberg, "The utility of the state-trait anger expression inventory with offenders," *International journal of offender therapy and comparative criminology*, vol. 46, pp. 364–78, 07 2002.

[5] C. Mathys, "Hgf toolbox - version 3.2.0," https://github.com/translationalneuromodeling/tapas/tree/master/HGF, 2010.

[6] J. Daunizeau, H. Den Ouden, M. Pessiglione, S. Kiebel, K. Stephan, and K. Friston, "Observing the observer (i): Meta-bayesian models of learning and decision-making," *PloS one*, vol. 5, p. e15554, 12 2010.

[7] H. Feldman and K. Friston, "Attention, uncertainty, and free-energy," *Frontiers in human neuroscience*, vol. 4, p. 215, 12 2010.

[8] T. Behrens, M. Woolrich, M. Walton, and M. Rushworth, "Learning the value of information in an uncertain world." *Nat Neurosci.*, vol. 10, pp. 1214–1221, 2007.

[9] M. J. Beal, "Variational algorithms for approximate bayesian inference," http://www.cse.buffalo.edu/faculty/mbeal/papers/beal03.pdf, 2003.

[10] K. Friston and K. Stephan, "Free energy and the brain," *Synthese*, vol. 159, pp. 417–458, 01 2008.

[11] C. Spielberger, *State-Trait Anxiety Inventory*, 01 2010, vol. 3.

http://tnutest.altervista.org

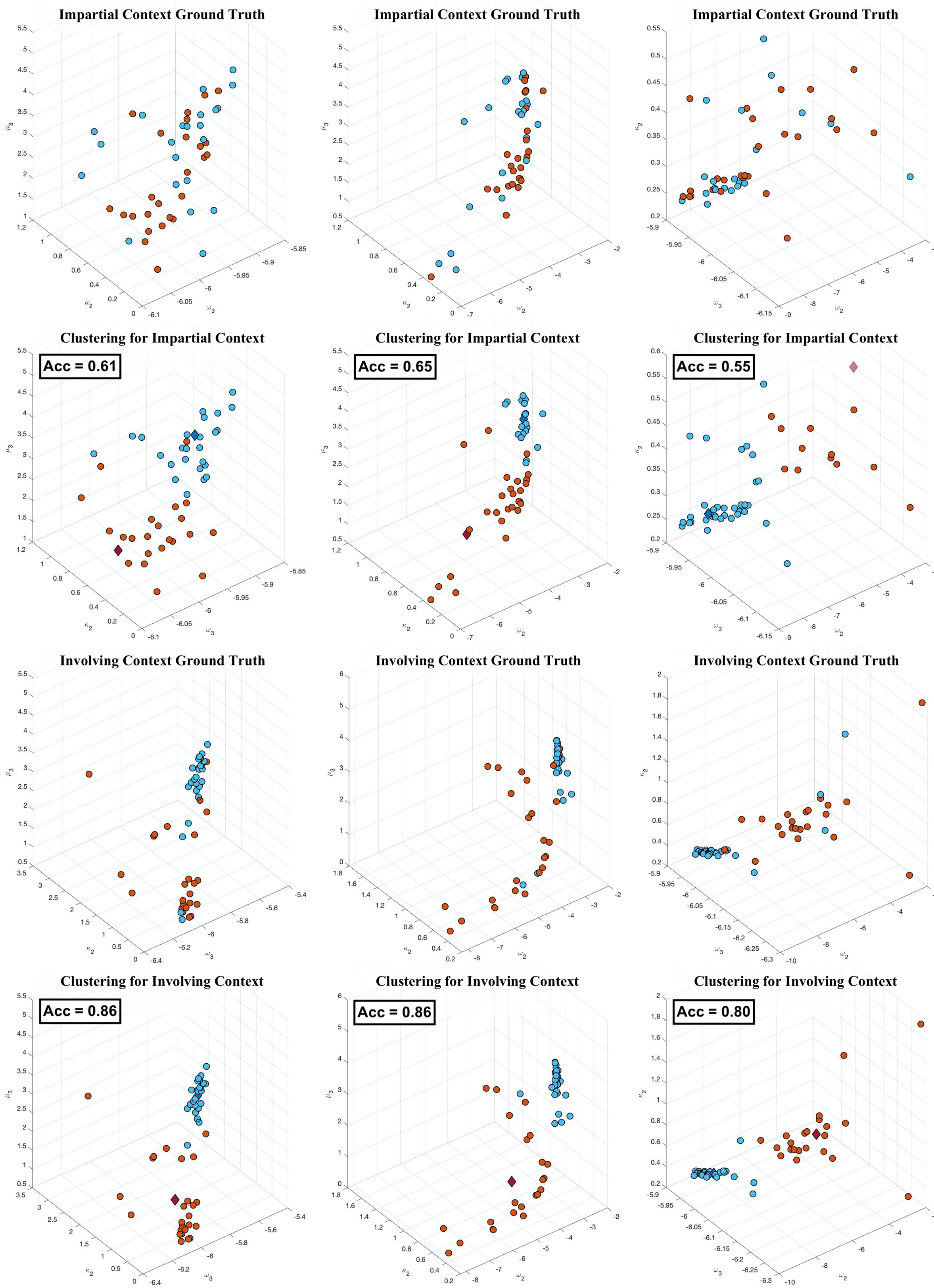

(a) $\omega_3, \kappa_2, \mu_3$ (b) $\omega_2, \kappa_2, \mu_3$ (c) $\omega_2, \omega_3, \kappa_2$

Fig. 9: Ground truth and K-Means clustering for different parameter estimations.